Scientific Reports

https://doi.org/10.1038/s41598-026-52206-2

Article in Press

Protein-free colorimetric biosensor for sensitive detection of HPV-18 mRNA via MNAzyme-driven catalytic hairpin assembly

Received: 31 October 2025

Accepted: 4 May 2026

Published online: 11 May 2026

Cite this article as: Wang Y., Wang C., Zhai L. *et al.* Protein-free colorimetric biosensor for sensitive detection of HPV-18 mRNA via MNAzyme-driven catalytic hairpin assembly. *Sci Rep* (2026). https://doi.org/10.1038/s41598-026-52206-2

Yingnan Wang, Chang Wang, Lin Zhai & Xiaoye Zhu

Protein-Free Colorimetric Biosensor for Sensitive Detection of HPV-18 mRNA via MNAzyme-Driven Catalytic Hairpin Assembly

Yingnan Wang[*1], Chang Wang[1], Lin Zhai[1], Xiaoye Zhu[1]

[1]Department of Gynecology, Ningbo Medical Center Lihuili Hospital, Ningbo, 315000, China

*Corresponding author: Yingnan Wang

E-mail: wangyingnan826@126.com

Abstract

Cervical cancer is significantly associated with persistent infection of human papillomavirus (HPV) type 18, making accurate detection of low-abundance HPV-18 mRNA crucial for diagnosis and treatment. Current nucleic acid detection methods are often limited by complex instrumentation, time-consuming procedures, or fluorophore modifications. To address this, we developed an enzyme-free colorimetric biosensor by integrating a multicomponent nucleic acid enzyme (MNAzyme) with catalytic hairpin assembly (CHA) for signal amplification. In this strategy, target recognition triggers the formation of an active MNAzyme that cleaves a substrate hairpin, initiating a CHA cascade which releases G-rich sequences. These sequences form G-quadruplexes with peroxidase-like activity, catalyzing the oxidation of colorless TMB into a soluble blue product, enabling both visual detection and spectrophotometric quantification at 650 nm. Under optimized conditions, the biosensor achieved a detection limit of 6.92 pM for HPV-18 mRNA, allowing naked-eye

identification of target levels as low as 10 pM. The platform exhibited high specificity and could be adapted to detect other HPV mRNA subtypes by simply modifying the recognition sequence. This work presents a universal, simplified, and sensitive colorimetric strategy with great promise for future development of point-of-care testing and viral analysis platforms.

Keywords: Cervical cancer; Catalytic hairpin assembly; MNAzyme; Colorimetric assay

Introduction

Cervical cancer is the fourth most common cancer among women worldwide, with mortality rates reaching up to 30 per 100,000 in underdeveloped regions and countries [1]. Extensive research has shown that HPV infection is the primary cause of cervical cancer, with more than 99% of invasive cervical cancers associated with high-risk HPV genotypes [2]. HPV is a non-enveloped DNA virus with a circular double-stranded, closed structure, and over 200 HPV subtypes have been identified to date [3]. Among these, HPV-18 is closely associated with approximately 70%-90% of cervical cancers [4]. Recent literature has also reported the detection of HPV-18 in sentinel lymph nodes of cervical cancer. Although HPV DNA testing has the drawback of false positives due to transient infections [5], HPV mRNA testing offers high specificity in detecting cervical intraepithelial lesions, thereby reducing the false positive rate [6]. Therefore, detecting HPV-18 mRNA is of significant importance for the diagnosis and treatment of cervical cancer.

A simple, simplified, and cost-effective biosensor for nucleic acid biomarker detection is crucial for early disease diagnosis and monitoring. Currently, various methods are widely used for HPV detection, such as high-performance liquid chromatography (HPLC) [7], electrochemical detection [8], fluorescence analysis [9], and colorimetric methods [10]. Each of these methods has its advantages but also presents certain limitations. For instance, HPLC typically requires bulky equipment, long washing times, specialized operators, and hazardous reaction conditions, which are not conducive to on-site testing [11, 12]. In contrast, colorimetric methods, with their visually readable results, portability, and ease of operation, are particularly suitable for the detection of HPV genes[13, 14]. However, traditional colorimetric methods often lack the sensitivity needed to detect trace targets due to the absence of signal amplification processes [15]. With the advancement of DNA nanotechnology, various signal amplification strategies have been developed, significantly enhancing the sensitivity of colorimetric methods [16]. Nonetheless, the low sensitivity of single amplification strategies still poses challenges for detecting trace targets [17]. To meet the demands for trace detection, methods combining multiple amplification strategies have garnered increasing attention, as they effectively address the limitations of single amplification strategies, thereby significantly improving detection sensitivity.

Functional nucleic acid technology has emerged as a prevalent approach for DNA analysis, attributed to its remarkable programmability, superior

detection capabilities, and straightforward synthesis processes [18, 19]. Multicomponent nucleic acid enzyme (MNAzyme), a nucleic acid-based catalytic molecule, facilitates the cyclic cleavage of specific substrate sequences, thereby enabling signal amplification, with the assistance of Mg^{2+} ions [20]. Several studies have demonstrated the integration of MNAzyme with various amplification techniques to boost detection sensitivity [21, 22]. Catalytic hairpin assembly (CHA) is an isothermal, protein-free signal amplification method that relies on DNA circuits for analyte detection [23, 24]. This method utilizes DNA circuits for isothermal amplification, initiating a signal cascade through branch migration between two metastable DNA hairpins. As a promising molecular amplifier, CHA has found extensive application in biosensor technology [25, 26]. The G-quadruplex/Hemin (GQ/Hemin) complex acts as a dependable signal output module for CHA reactions, suitable for direct colorimetric analysis due to its thermal stability and ease of preparation and modification [26]. Upon the formation of the GQ/Hemin complex by the interaction of a G-quadruplex with Hemin, it can catalyze redox reactions of substrates like 3,3',5,5'-tetramethylbenzidine (TMB) and ABTS in the presence of hydrogen peroxide, causing notable changes in the solution's color and absorption spectrum [27].

In this research, we designed a protein-free colorimetric biosensing system by combining MNAzyme and CHA to detect HPV-18 mRNA. Upon specific recognition of HPV-18 mRNA by the MNAzyme, an active MNAzyme

complex is formed, which cleaves H1. The cleavage event triggers a subsequent CHA cascade, leading to the sequential unfolding of DNA hairpins H2 and H3. This chain of cyclic reactions amplifies the signal by producing a significant quantity of G-quadruplex structures. In the presence of Hemin, the self-assembled GQ/Hemin complex mimics the activity of horseradish peroxidase, catalyzing the transformation of the colorless substrate TMB into a soluble blue product. The resultant color change and optical density variations in the solution provide a straightforward method for both qualitative and quantitative sample analysis. Therefore, we believe that combining MNAzyme cleavage with the CHA strategy not only enhances detection sensitivity but also provides a novel approach for the detection of trace targets using multiple amplification strategies.

Materials and methods

Cell Line and Cell Culture

HEK293 cells were cultured in DMEM medium (Gibco, USA) supplemented with 10% fetal bovine serum (FBS) and 100 U/mL penicillin-streptomycin. The culture conditions were 37 ℃ with 5% CO_2. When the cells reached 60-80% confluence, the medium was replaced with DMEM without FBS. After approximately 48 hours of culture, the HEK293 cells was collected for subsequent experiments.

Materials and Reagents

The synthetic oligonucleotides utilized in this study were commercially obtained from Sangon Biotech (China) Co., Ltd., with corresponding

sequences provided in Table S1. Essential biochemical reagents including PBS, KCl, NaCl, $MgCl_2 \cdot 6H_2O$, 6× DNA loading buffer, and PAGE Pre-Solution were acquired from Solarbio Science & Technology Co., Ltd. For buffer preparation, 1 M Tris-HCl solution (pH 7.4) was purchased from Beyotime Institute of Biotechnology (China). Critical reaction components comprising 3,3′,5,5′-tetramethylbenzidine (TMB), Hemin, and the N,N,N′,N′-Tetramethylethylenediamine (TEMED) were supplied by Aladdin Reagent (China) Co., Ltd.. All remaining reagents were of analytical grade and employed without further purification.

Probe Design Rationale

The design of oligonucleotide probes (Part1, Part2, H1, H2, H3) followed established principles for MNAzyme and CHA systems to ensure efficient target recognition, cleavage, and signal amplification. The split MNAzyme sequences in Part1 and Part2 were derived from the 10-23 DNAzyme motif, with arm lengths of 8–10 nucleotides selected based on prior studies to ensure stable hybridization with target mRNA while maintaining catalytic activity upon assembly [28]. The substrate H1 incorporates a single ribonucleotide (rU) flanked by a guanine (rG) to form an rG–rU dinucleotide cleavage site, which is efficiently recognized and cleaved by the assembled MNAzyme in the presence of Mg^{2+}. For the CHA component, the sequences of H2 and H3 were designed using NUPACK (http://www.nupack.org) to minimize secondary structure interference and to maintain metastable states in the absence of the initiator sDNA1. Stem regions were optimized

to exhibit ΔG values between -6 and -8 kcal/mol, preventing spontaneous opening while allowing efficient strand displacement during CHA. Additionally, H2 contains a G-rich track (GGGT) that, upon release, forms a stable parallel G-quadruplex structure capable of binding hemin and exhibiting peroxidase-mimicking activity for colorimetric signal output.

Fluorescence assay validation of MNAzyme

To validate the structural integrity of the MNAzyme assembly, we engineered the terminal regions of H1 with FAM/BHQ1 fluorophore-quencher pairs. Reactions were conducted in Tris-HCl buffer (pH 7.4) to maintain physiological compatibility and catalytic efficiency. Part1 and Part2 were denatured in PBS buffer at 95 ℃ for 5 min and slowly cooled (0.5 ℃/min) to room temperature for structural optimization. The preassembled system was then combined with 1 nM HPV18 mRNA and annealed at 25 ℃ for 60 min to achieve precise MNAzyme configuration, a temperature chosen to preserve high catalytic specificity. Subsequently, predetermined concentrations of the modified H1 probe were introduced into the reaction system and maintained at 25 ℃ for 60 min to facilitate molecular recognition. Fluorescence quantification was performed using a Hitachi F-7000 spectrophotometer configured with FAM-specific parameters: excitation λ = 485 nm, emission λ = 520 nm, with 5 nm slit widths for both channels.

Agarose Gel Electrophoresis

The DNA samples were supplemented with 2 μL of 100× SYBR Gold nucleic

acid stain and 2 μL of 6× DNA loading buffer to prepare electrophoretic mixtures. Electrophoretic separation was performed in 3% agarose matrix (w/v) submerged in 1 × TAE running buffer (40 mM Tris-acetate, 2 mM EDTA, pH 8.5). Electrophoresis parameters were maintained at 110 V constant voltage for 60 min. Following SYBR Gold staining, nucleic acid bands were visualized under UV illumination using a Bio-Rad GelDoc XR documentation system (Bio-Rad Laboratories, USA).

Colorimetric measurements

Reactions were performed in Tris-HCl buffer (pH 7.4) containing 20 mM KCl to maintain physiological compatibility and ensure robust catalysis [29, 30]. Prior to hybridization, Part1 and Part2 underwent thermal denaturation in PBS buffer (95 ℃, 5 min) followed by gradual cooling (0.5 ℃/min) to ambient conditions for structural optimization. The preassembled system was subsequently supplemented with 1 nM HPV18 mRNA and subjected to molecular annealing (25 ℃, 60 min) to ensure precise MNAzyme configuration (this temperature was optimized to maintain high catalytic specificity). For hairpin structure preparation, H1/H2/H3 oligonucleotides were heated at 95 ℃ for 5 min in Tris-HCl buffer, followed by slow annealing at a cooling rate of 1 ℃/min to obtain the designed hairpin structures. The catalytic cascade was initiated by introducing 5 μL of 200 nM preconditioned H1, followed by 30 min incubation under isothermal conditions (25 ℃). Subsequent introduction of 10 μL of 200 nM H2 and H3 probes enabled chain hybridization at 37 ℃ for 60 min. The chromogenic

phase commenced with sequential addition of hemin (200 nM final concentration), 30 μL TMB liquid substrate (0.1 mg/mL TMB) and 20 μL of 0.03% H_2O_2, allowing 15 min dark-phase enzymatic oxidation. Spectral characterization was conducted at ambient temperature using full-wavelength scanning (300-700 nm) with peak absorption quantification at 650 nm.

Results

Principle of the assay

The design strategy for protein-free colorimetric detection of HPV18 mRNA based on MNAzyme cleavage and CHA dual signal amplification is illustrated in Fig. 1. The detection system utilizes two nucleic acid probes (Part1 and Part2). Specifically, two fully complementary DNA sequences and two split MNAzyme sequences are integrated into Part1 and Part2, respectively, allowing them to hybridize and form a duplex DNA. In the absence of HPV18 mRNA, Part1 and Part2 cannot form a complete MNAzyme. However, when HPV18 mRNA is introduced, it brings the split fragments of Part1 and Part2 into close proximity, inducing the formation of an active MNAzyme capable of cleaving the target substrate. In the presence of Mg^{2+}, the active MNAzyme efficiently cleaves substrate H1, generating segment DNA (sDNA 1), which serves as a new activator unit for triggering subsequent CHA reactions. In brief, sDNA 1 can hybridize with hairpin H2, releasing the G-rich sequence of H2. Subsequently, H2 can hybridize with hairpin H3, and upon the addition of hemin, form a G-

quadruplex/hemin complex that exhibits horseradish peroxidase-like activity, efficiently catalyzing the oxidation of TMB into a colored product (oxTMB). The opened H2 then binds with H3 to form an H2–H3 complex, releasing sDNA 1 to initiate the next cycle, thereby continuing to trigger additional CHA reactions and resulting in a signal cascade amplification. Through these cycles, a protein-free signal amplification method is successfully established for the sensitive and visual detection of HPV18 mRNA.

Feasibility of analyzing HPV18 mRNA

The proposed detection strategy relies on the target-triggered formation of an active MNAzyme and its subsequent cleavage of the substrate. Therefore, Native-PAGE was first performed to verify these specific molecular events (Fig. S1). As shown in the gel electrophoresis results, the individual components and partial mixtures migrated rapidly (Lanes 1-4). However, the introduction of HPV18 mRNA successfully induced the hybridization of Part1 and Part2, forming a distinctly retarded band representing the assembled active MNAzyme ternary complex (Lane 5). To validate the catalytic cleavage, substrate H1 was introduced. In the presence of the essential cofactor Mg^{2+}, the complete H1 band (55 nt) was markedly consumed, accompanied by the clear emergence of a new dense band at approximately 25-28 nt, corresponding to the expected cleavage products (Lane 8). Conversely, no cleavage occurred in the absence of Mg^{2+} (Lane 7). This direct evidence validates the successful target-recognition and the specific H1 cleavage capability of our design. Furthermore, this cleavage

event was dynamically confirmed in solution using a FRET-based fluorescence assay (Fig. S2). By modifying the termini of H1 with a FAM/BHQ1 pair, the intact H1 remained quenched due to proximity. Upon adding the target mRNA, the fully assembled MNAzyme cleaved H1, separating the fluorophore and quencher, which led to a significant recovery of the fluorescence signal.

Following the successful upstream cleavage, the released segment DNA (sDNA 1) proceeds to trigger the downstream catalytic hairpin assembly (CHA). To monitor this overall cascaded signal amplification, we recorded the UV-vis absorption spectra of the solutions under various conditions (Fig. 2A and 2B). When either HPV18 mRNA or Part1 was absent, only a minor absorption signal was detected, indicating that an active MNAzyme was not generated, thereby preventing the initiation of the CHA cascade. Similarly, the absence of H1, H2, or H3 resulted in low absorption signals akin to the control group (curve a). In striking contrast, the complete sensing system containing HPV18 mRNA (curve f) exhibited a massive increase in the absorption signal. This pronounced signal boost demonstrates that the target-induced sDNA 1 successfully opened hairpin H2, promoting the autonomous cyclic formation of the H2-H3 complex. This amplification process releases a substantial amount of G-rich sequences that fold into G-quadruplex/Hemin complexes. Acting as horseradish peroxidase mimics, these abundant complexes efficiently catalyze the oxidation of TMB, producing the intense colorimetric signal and confirming the excellent

analytical feasibility of the entire system.

Optimization of the Critical Parameters

To optimize the analytical performance of the MNAzyme-driven CHA detection system, the signal-to-background ratio (A/A0) was used to identify the best experimental conditions, where A is the absorbance intensity in the presence of the target HPV18 mRNA, and A0 is the absorbance intensity in its absence (blank). This included determining the optimal concentrations of Mg^{2+}, H1, H2, and H3, as well as the ideal reaction time for the CHA system. Here, A and A0 represent the absorbance intensities with and without the target HPV18 mRNA, respectively. Mg^{2+} not only stabilizes DNA hybridization but also enhances MNAzyme catalytic activity [31], significantly affecting the A/A0 ratio. As shown in Fig. 3A, an Mg^{2+} concentration of 10 mM notably increased the A/A0 value, leading to its selection for further tests. H1 is crucial for the system's analytical performance. While a sufficient amount of H1 is necessary for effective cycling, higher concentrations can cause significant background signals due to nonspecific H1-H2 interactions. Therefore, for detecting 0.1 nM HPV18 mRNA, 100 nM of H1 was determined to be optimal, as illustrated in Fig. 3B. The concentrations of H2 and H3 greatly influence the CHA system's amplification efficiency. Low levels of these components can reduce efficiency, while excessive amounts may form a stable H2–H3 duplex, increasing background (A0). Fig. 3C indicates that 200 nM of both H2 and H3 are optimal, and these concentrations were selected to ensure high

sensitivity in subsequent experiments. The CHA reaction time, a critical factor, affects the stability and interaction of H2 and H3. Fig. 3D shows that the A/A0 ratio increases with reaction time, reaching saturation at 60 minutes. Thus, 60 minutes was chosen as the optimal CHA reaction time.

Sensitivity for the sensing system

After optimizing the critical reaction parameters for the MNAzyme-driven CHA detection system, we tested various concentrations of HPV18 mRNA (ranging from 1 pM to 10 nM) to assess the effectiveness of this colorimetric detection method. As illustrated in Fig. 4, without HPV18 mRNA, the solution remained colorless. However, as the concentration of HPV18 mRNA increased, the absorbance at 650 nm in the UV-visible spectrum rose, and the solution turned increasingly blue, indicating enhanced catalytic activity of the self-assembled GQ/Hemin complex. Our colorimetric method can visually detect HPV18 mRNA concentrations as low as 10 pM (Fig. 4A). There was a linear positive correlation between absorbance and the logarithm of HPV18 mRNA concentration from 10 pM to 50 nM (R^2 = 0.957), with the linear regression equation given by $Y = 0.0975*\lg(C_{HPV18\ mRNA}) + 0.2559$, where Y is the absorbance at 650 nm and CHPV18 mRNA is the target mRNA concentration. The LOD was determined by calculating the signal of the blank plus three times the standard deviation ($Y_{LOD}=\bar{Y}_{blank}+3\sigma$), and substituting this absorbance value into the regression equation to solve for the concentration (Fig. 4B). These LOD results and the standard curve confirm the method's good

sensitivity.

Absorbance plots of different samples at 650 nm

We further assessed the anti-interference capabilities of the MNAzyme-driven CHA dual-signal amplification strategy by introducing varying concentrations of BSA (0, 0.5%, 5%, and 10%) into the Tris-HCl buffer. As shown in Fig. 5A, the method achieved a relative standard deviation (RSD) of approximately 5.11% (n = 3) when detecting HPV18 mRNA, demonstrating exceptional anti-interference performance in complex environments. To test the long-term storage stability, we stored the main analytical reagents (H1, H2, and Part1 and Part2 sequences) at -20 ℃ (Fig. 5B). The results indicated that, with proper storage (minimizing freeze-thaw cycles), the DNA sequences retained appreciable stability and analytical performance over time. The method's stability and strong detection performance are largely due to its homogeneous analysis approach and the inherent stability of the nucleic acid components. Additionally, we evaluated the system's selectivity while maintaining a low detection limit. To test specificity, we replaced the HPV18 RNA target with a single-base mismatch, a double-base mismatch, HPV16 RNA, and a non-complementary sequence. Fig. 5C shows that even at concentrations five times higher than HPV18 mRNA, the absorbance intensity for single-base mismatch (mm1), double-base mismatch (mm2), scrambled sequence (scramble), or HPV16 mRNA did not change significantly.

Real sample application

To validate the applicability of the MNAzyme-driven CHA detection system for detecting HPV18 mRNA in real samples, different concentrations of target RNA were added to total RNA extracted from HEK293 cells, which represent a complex matrix of real samples. The proposed detection system was used to analyze the absorbance of each group. As shown in Fig. 6, the signal for different target nucleic acid sequence concentrations in the presence of total RNA extract was comparable to that without the total RNA extract. Despite the presence of 1 μg/mL total RNA extract, the analysis of 0.1 nM, 1 nM, and 10 nM target RNA showed recovery rates of 103%, 98%, and 95%, respectively. To assess the robustness and practical reliability of the biosensor, inter-batch reproducibility was evaluated. A fixed concentration of HPV-18 mRNA (1 nM) was detected using three independently prepared batches of the core probes (Part1/Part2, H1, H2, H3) on different days. The average absorbance at 650 nm was 0.52 with a standard deviation of 0.04, yielding an RSD of 7.7% (Table S2). This result indicates acceptable reproducibility between different assay preparations. It should be noted that the current ‘real sample’ validation utilized a cellular total RNA background. While this demonstrates robustness against nonspecific nucleic acid interference, clinical specimens such as cervical swabs or biopsies contain a more complex mixture of biomolecules (e.g., proteins, mucins, potential PCR inhibitors). Furthermore, the clinical relevance of the achieved pM-level sensitivity needs to be established through testing against patient samples with known viral loads. Therefore,

future work will focus on validating the assay in such authentic clinical matrices to fully assess its diagnostic potential.

Discussion

The study presents a novel protein-free colorimetric detection method for HPV18 mRNA, utilizing a MNAzyme cleavage and CHA dual signal amplification strategy. The results demonstrate the potential of this approach for sensitive and specific nucleic acid detection, providing significant advancements in the field of molecular diagnostics. The design of the assay leverages the unique properties of MNAzymes and CHA, creating a robust system capable of amplifying weak signals without the need for enzymatic reactions. The feasibility tests indicated that HPV18 mRNA effectively triggered the formation of an active MNAzyme, which subsequently initiated the CHA process. The use of electrophoresis and FRET-based assays confirmed the successful assembly and activity of the MNAzyme, providing evidence for the precise molecular interactions and the efficiency of the cleavage and amplification processes. The optimization of key parameters, such as Mg^{2+} concentration and the concentrations of H1, H2, and H3, was critical in enhancing the assay's performance. The established optimal conditions allowed for a significant increase in the A/A0 value, indicating improved sensitivity and robustness of the detection system. The system demonstrated a lower detection limit of 6.92 pM for HPV18 mRNA, showcasing its ability to detect even trace amounts of target mRNA.

To contextualize the performance of our biosensor, we compare it with other representative methods for HPV nucleic acid detection (Table S3). While techniques like CRISPR-Cas and RT-qPCR offer exceptional sensitivity, they require specialized enzymes, precise temperature control, and complex instrumentation. Electrochemical and fluorescence-based CHA assays provide high sensitivity but often depend on modified electrodes or fluorophore labels. In contrast, the present MNAzyme-driven CHA colorimetric assay achieves pM-level sensitivity without any protein enzymes or sophisticated equipment. Its primary advantages lie in operational simplicity, visual readout capability, and being entirely protein-free, making it a promising candidate for resource-limited settings or point-of-care screening where ease of use and cost are paramount. This high sensitivity is attributed to the synergistic effect of MNAzyme and CHA, which amplifies the signal through repeated cycles. The specificity tests revealed that the detection system effectively discriminates between the target HPV18 mRNA and non-target sequences, including single and double mismatches, as well as other HPV types. This specificity is crucial for accurate diagnostics, minimizing false positives. The anti-interference experiments further demonstrated the system's resilience in complex biological matrices, maintaining performance despite the presence of potential confounding factors. Additionally, the long-term stability of the analytical reagents under appropriate storage conditions supports the practical applicability of this method for routine use. The successful

detection of HPV18 mRNA in the presence of total RNA extracted from HIK293 cells underscores the method's applicability in real-world scenarios. While the total assay time of approximately 2 hours is longer than some ideal POC formats, it is notably shorter and far less labor-intensive than gold-standard methods like quantitative reverse transcription PCR (qRT-PCR). The simplicity, isothermal nature, and elimination of enzymatic steps constitute the primary advantages of this platform in a laboratory or resource-limited setting.

Despite the promising results, this study has several limitations that point to future research directions. First, the detailed reaction kinetics (e.g., turnover number of the MNAzyme, amplification folds of the CHA circuit) were not quantified, transitioning the assay to a single, constant incubation temperature would greatly enhance its simplicity and suitability for resource-limited settings. Future work will explore the feasibility of performing both the MNAzyme cleavage and CHA amplification steps at a unified isothermal condition without compromising sensitivity or specificity. Second, while high specificity was shown against synthetic mismatches and another high-risk HPV genotype (HPV-16), validation using clinically prevalent HPV-18 variants (e.g., E6/E7 splice variants) and in co-infection scenarios is necessary for clinical translation. Additionally, a more comprehensive specificity profile could be obtained by testing against a broader panel of unrelated nucleic acids and evaluating the assay’s performance under conditions that simulate sample degradation, such as in

the presence of RNases. Third, direct benchmarking of the detection sensitivity and specificity against the clinical gold standard, qRT-PCR, using a large set of patient samples, is the essential next step to establish clinical utility. Addressing these points will be the focus of our ongoing work to advance this biosensing platform toward practical diagnostic applications. Furthermore, to enhance its suitability for true point-of-care testing, future work will focus on reducing the total assay time. This could be achieved by engineering probes with faster hybridization kinetics, employing elevated but isothermal reaction temperatures, or integrating the assay into a microfluidic or lateral flow device to accelerate mass transport and signal development.

Conclusion

Overall, we have developed a protein-free dual-signal amplification strategy based on MNAzyme and CHA for the pM-level sensitivity detection of HPV18 mRNA, which offers several significant advantages. First, the protein-free amplification approach overcomes the drawbacks associated with protein enzyme use, such as high cost, short shelf life, and insufficient stability. Second, the method is portable by design, easy to operate, requires simple instrumentation, and allows for convenient visual readout. Third, by merely adjusting the recognition segments, the sensing system can be adapted to a broader range of other targets. We believe that this developed biosensing strategy provides a simple and stable platform for sensitive and convenient miRNA detection, holding great potential for the

detection of nucleic acid analytes in biomedical research and as a foundational technology for future clinical diagnostic applications.

Data availability Statement The datasets generated during the study are available from the corresponding author on reasonable request.

Author contributions Chang Wang: investigation, writing of original draft and visualization. Lin Zhai: investigation. Xiaoye Zhu: supervision. Yingnan Wang: conceptualization, methodology, supervision, project administration and writing—review and editing.

Funding This study was supported by the Ningbo Science and Technology Plan Project (202003N4286).

Declarations

Competing interests The authors declare no competing interests.

Supporting Information Additional supporting information can be found online in the Supporting Information section. (Supporting Information) Table S1. Oligonucleotide sequences involved in the experiment. Table S2. Inter-batch reproducibility. Table S3. Comparison of different methods for HPV nucleic acid detection. Fig. S1. The polyacrylamide gel electrophoresis characterization of MNAzyme assembly and catalytic cleavage. Fig. S2. Fluorescence emission spectra of the process of MNAzyme formation and target addition.

References

1. Xia C, Basu P, Kramer BS, Li H, Qu C, Yu XQ, et al. Cancer screening in China: a steep road from evidence to implementation. Lancet Public Health.

2023;8(12):e996-e1005. doi: 10.1016/s2468-2667(23)00186-x.

2. Frazer IH, Leggatt GR, Mattarollo SR. Prevention and treatment of papillomavirus-related cancers through immunization. Annu Rev Immunol. 2011;29:111-38. doi: 10.1146/annurev-immunol-031210-101308.

3. Mandic A, Vujkov T. Human papillomavirus vaccine as a new way of preventing cervical cancer: a dream or the future? Ann Oncol. 2004;15(2):197-200. doi: 10.1093/annonc/mdh043.

4. de Sanjose S, Quint WG, Alemany L, Geraets DT, Klaustermeier JE, Lloveras B, et al. Human papillomavirus genotype attribution in invasive cervical cancer: a retrospective cross-sectional worldwide study. The Lancet Oncology. 2010;11(11):1048-56. doi: 10.1016/s1470-2045(10)70230-8.

5. A PCM, A MA, a LP-CM, A SPC, a RMC, a MTH-H, et al. Diagnosis of Transient/Latent HPV Infections - A Point of View! Archives of Medical Research. 2018;49(5):293-6.

6. Zhang SK, Guo Z, Wang P, Kang LN, Jia MM, Wu ZN, et al. The Potential Benefits of HPV E6/E7 mRNA Test in Cervical Cancer Screening in China. Frontiers in oncology. 2020;10:533253. doi: 10.3389/fonc.2020.533253.

7. Schott M, Vehlow A, Benka M, Lagies S, Kammerer B, Rieckmann T, et al. Aqueous extracts from Dioscorea sansibarensis Pax show cytotoxic and radiosensitizing potential in 3D growing HPV-negative and HPV-positive human head and neck squamous cell carcinoma models. Biomedicine & pharmacotherapy = Biomedecine & pharmacotherapie. 2024;179:117305. doi: 10.1016/j.biopha.2024.117305.

8. Izadi N, Strmiskova J, Anton M, Hausnerova J, Bartosik M. LAMP-based electrochemical platform for monitoring HPV genome integration at the mRNA level associated with higher risk of cervical cancer progression. Journal of medical virology. 2024;96(10):e70008. doi: 10.1002/jmv.70008.

9. Chen Y, Wang X, Zhang J, Jiang Q, Qiao B, He B, et al. Split crRNA with CRISPR-Cas12a enabling highly sensitive and multiplexed detection of RNA and DNA. Nat Commun. 2024;15(1):8342. doi: 10.1038/s41467-024-52691-x.

10. Cao Y, Lin H, Lu X, Wu X, Zhu Y, Zhao Z, et al. Benchtop to at-home test: Amplicon-depleted CRISPR-regulated loop mediated amplification at skin-temperature for viral load monitoring. Biosens Bioelectron. 2025;267:116866. doi: 10.1016/j.bios.2024.116866.

11. Yan Y, Liu JH, Li RS, Li YF, Huang CZ, Zhen SJ. Carbon dots synthesized at room temperature for detection of tetracycline hydrochloride. Analytica chimica acta. 2019;1063:144-51. doi: 10.1016/j.aca.2019.02.047.

12. Zhang Z, Tian Y, Huang P, Wu FY. Using target-specific aptamers to enhance the peroxidase-like activity of gold nanoclusters for colorimetric detection of tetracycline antibiotics. Talanta. 2020;208:120342. doi: 10.1016/j.talanta.2019.120342.

13. Kwon YS, Ahmad Raston NH, Gu MB. An ultra-sensitive colorimetric detection of tetracyclines using the shortest aptamer with highly enhanced affinity. Chemical communications (Cambridge, England). 2014;50(1):40-2. doi: 10.1039/c3cc47108j.

14. Jiang C, Huang Y, He T, Huang P, Lin J. A dual-round signal

amplification strategy for colorimetric/photoacoustic/fluorescence triple read-out detection of prostate specific antigen. Chemical communications (Cambridge, England). 2020;56(36):4942-5. doi: 10.1039/d0cc01086c.

15. Xu S, Ouyang W, Xie P, Lin Y, Qiu B, Lin Z, et al. Highly Uniform Gold Nanobipyramids for Ultrasensitive Colorimetric Detection of Influenza Virus. Analytical chemistry. 2017;89(3):1617-23. doi: 10.1021/acs.analchem.6b03711.

16. Zheng AX, Li J, Wang JR, Song XR, Chen GN, Yang HH. Enzyme-free signal amplification in the DNAzyme sensor via target-catalyzed hairpin assembly. Chemical communications (Cambridge, England). 2012;48(25):3112-4. doi: 10.1039/c2cc30305a.

17. Sun X, Wang S, Zhang Y, Tian Y, Zhou N. Ultrasensitive detection of DNA based on target-triggered hairpin assembly and exonuclease-assisted recycling amplification. Sensors and Actuators B Chemical. 2017;252.

18. Jie H, Junyi W, Yan D, Jingyao Y, Zhe W, Xiaoxin Z, et al. Homogeneous, Simple, and Direct Analysis of Exosomal PD-L1 via Aptamer-Bivalent-Cholesterol-Anchor Assembly of DNAzyme (ABCzyme) for Tumor Immunotherapy. Analytical chemistry. 2023;95(17). doi: 10.1021/acs.analchem.2c05461.

19. Yuxiong L, Yingying S, Wenjie L, Jianna Y, Guoxing J, Wen L, et al. Enzyme-free dual-amplification assay for colorimetric detection of tetracycline based on Mg(2+)-dependent DNAzyme assisted catalytic hairpin assembly. Talanta. 2022;241:123214. doi:

10.1016/j.talanta.2022.123214.

20. Mokany E, Bone SM, Young PE, Doan TB, Todd AV. MNAzymes, a versatile new class of nucleic acid enzymes that can function as biosensors and molecular switches. Journal of the American Chemical Society. 2010;132(3):1051-9. doi: 10.1021/ja9076777.

21. Safdar S, Lammertyn J, Spasic D. RNA-Cleaving NAzymes: The Next Big Thing in Biosensing? Trends Biotechnol. 2020;38(12):1343-59. doi: 10.1016/j.tibtech.2020.04.012.

22. Kim SH, Kim Y, Kim S, Lee ES, Cha BS, Park KS. MNAzyme-Assisted Nucleic Acid Lateral Flow Assay for Cost-Effective, On-Site Mercury Detection. Biosensors (Basel). 2024;14(10). doi: 10.3390/bios14100454.

23. Li R, Chen Y, Pan R, Hu S, Zhao S, Tian J, et al. Single-Cell Multiplexed Signal Amplification Strategy Based on Catalytic Hairpin Self-Assembly and CRISPR/Cas12a for Exploring the Relationship between lncRNA HOTAIR and miRNA-122 in Individual Hepatocytes. Analytical chemistry. 2024;96(45):18096-103. doi: 10.1021/acs.analchem.4c03974.

24. Chen J, Pan J, Chen S. A label-free and enzyme-free platform with a visible output for constructing versatile logic gates using caged G-quadruplex as the signal transducer. Chemical science. 2018;9(2):300-6. doi: 10.1039/c7sc04007e.

25. Bai G, Fan Z, Zhao X, Dong Y, Tan C, Bai L, et al. Highly sensitive and portable detection of PD-L1(+) exosomes using a smartphone-assisted colorimetric sensor. Biosens Bioelectron. 2025;286:117592. doi:

10.1016/j.bios.2025.117592.

26. Weng Q, Li H, Fan Z, Dong Y, Qi Y, Wang P, et al. Enzyme-free and rapid colorimetric analysis of osteopontin via triple-helix aptamer probe coupled with catalytic hairpin assembly reaction. Analytica chimica acta. 2024;1312:342764. doi: 10.1016/j.aca.2024.342764.

27. Xi H, Juhas M, Zhang Y. G-quadruplex based biosensor: A potential tool for SARS-CoV-2 detection. Biosens Bioelectron. 2020;167:112494. doi: 10.1016/j.bios.2020.112494.

28. Gerasimova YV, Kolpashchikov DM. Nucleic acid detection using MNAzymes. Chemistry & biology. 2010;17(2):104-6. doi: 10.1016/j.chembiol.2010.02.003.

29. Pavlov V, Xiao Y, Gill R, Dishon A, Kotler M, Willner I. Amplified chemiluminescence surface detection of DNA and telomerase activity using catalytic nucleic acid labels. Analytical chemistry. 2004;76(7):2152-6. doi: 10.1021/ac035219l.

30. Ito Y, Hasuda H. Immobilization of DNAzyme as a thermostable biocatalyst. Biotechnology and bioengineering. 2004;86(1):72-7. doi: 10.1002/bit.20041.

31. Yang K, Wang H, Ma N, Zeng M, Luo H, He D. Programmable Target-Initiated DNAzyme Walker Walking along a Spatially Isolated and Highly Hybridizable Substrate Track on a Nanoparticle Surface. ACS applied materials & interfaces. 2018;10(51):44546-53. doi: 10.1021/acsami.8b16408.

Figure legends

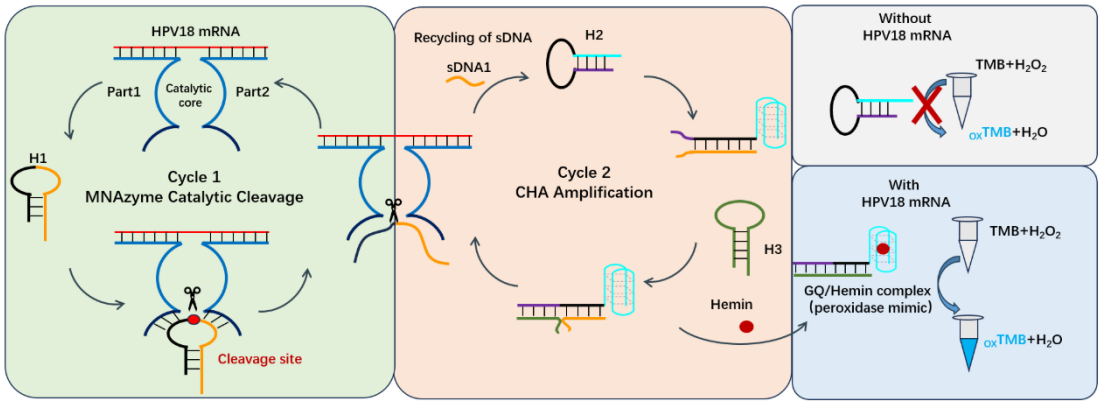

Fig. 1 Schematic diagram of the operating principle for HPV18 mRNA analysis.

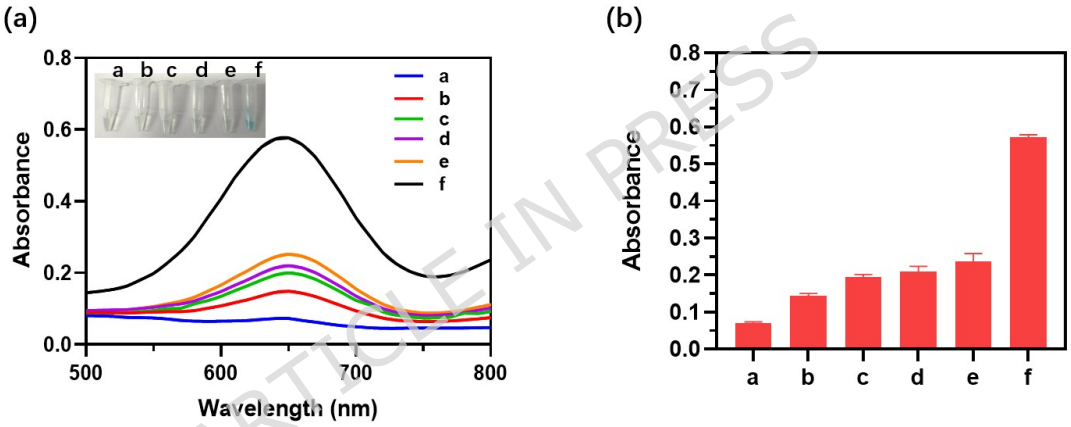

Fig. 2 Absorbance spectra of the solution under different treatment conditions (A) and statistical analysis of absorbance at 650 nm (B). Grouping: (a) Without HPV18 mRNA, (b) Without Part1, (c) Without H1, (d) Without H2, (e) Without H3, (f) With HPV18 mRNA and all probes. The concentrations of HPV18 mRNA, Part1, Part2, H1, H2, and H3 are 0.1 nM, 20 nM, 20 nM, 100 nM, 200 nM, and 200 nM, respectively.

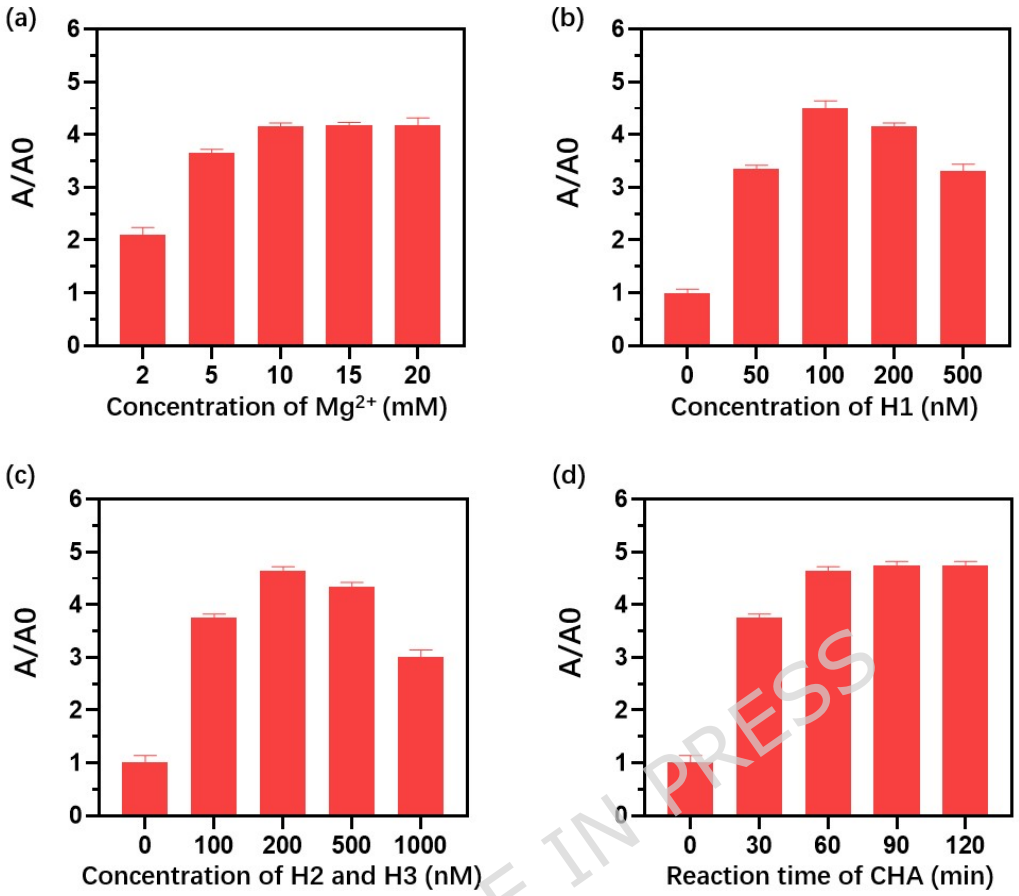

Fig. 3 Optimization results of different influencing factors: (A) Mg^{2+} concentration, (B) H1 concentration, (C) H2 and H3 concentrations, (D) reaction time of the CHA system.

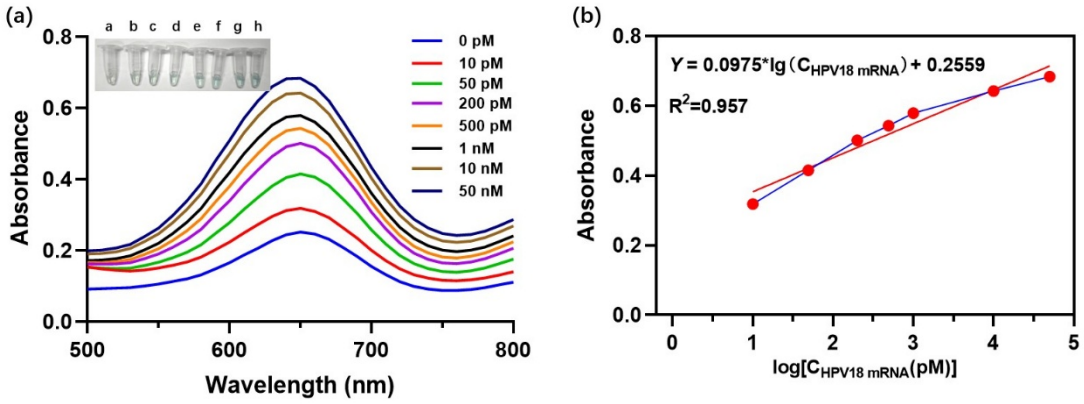

Fig. 4 (A) Absorption spectra for detecting different concentrations of HPV18 mRNA. (B) Standard curve of absorbance for HPV18 mRNA ranging from 10 pM to 50 nM using the MNAzyme-driven CHA detection system.

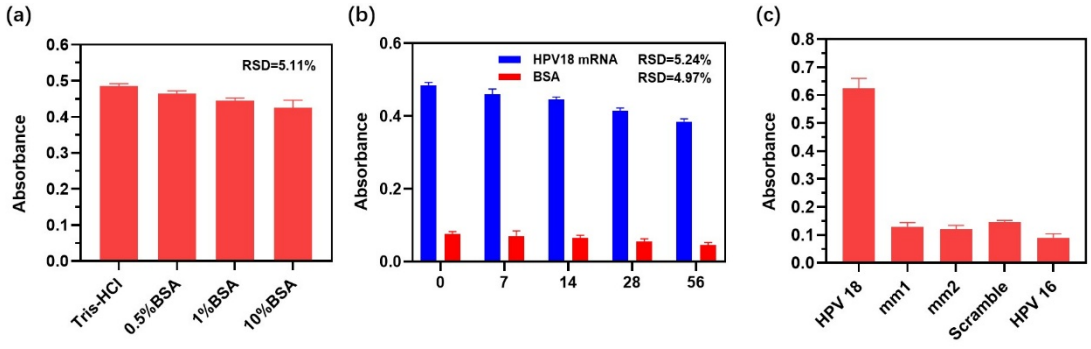

Fig. 5 (A) HPV18 mRNA in different amounts of added BSA (0, 0.5%, 5% and 10%) was detected by MNAzyme-driven CHA dual-signal amplification strategy. (B) The effect of the storage cycle of the main analytical reagents of MNAzyme-driven CHA dual-signal amplification strategy on the detection efficacy of the strategy. (C) The selectivity of the MNAzyme-driven CHA detection system was evaluated in the presence of a perfectly matched target (HPV18), a single-base mismatch (mm1), a double-base mismatch (mm2), a scrambled RNA sequence (scramble), or an HPV-16 mRNA sequence (HPV16).

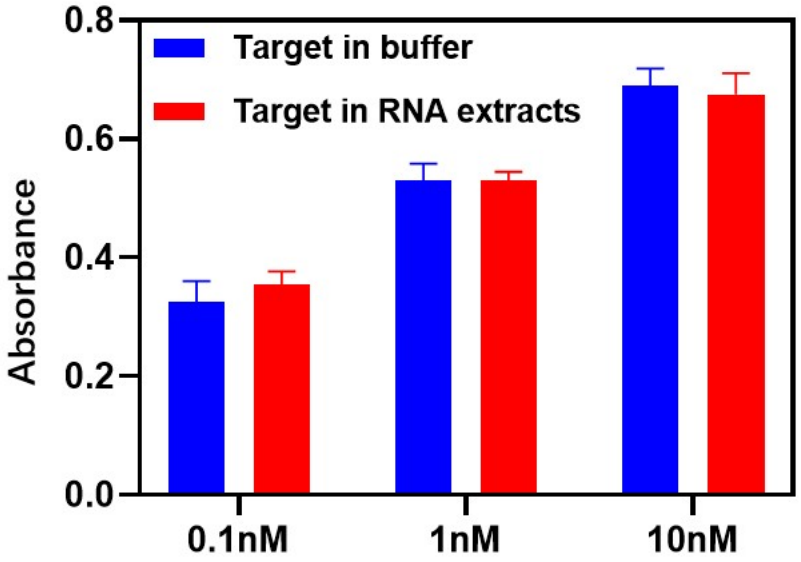

Fig. 6 Absorbance of different target nucleic acid sequence concentrations (0.1, 1, and 10 nM) in the presence or absence of 1 μg/mL total RNA extract.